NANO LETTERS

Letter

pubs.acs.org/NanoLett

Single Molecules Trapped by Dynamic Inhomogeneous Temperature Fields

Marco Braun,[†] Andreas P. Bregulla,[†] Katrin Günther,[‡] Michael Mertig,[‡,§] and Frank Cichos*,[†]

[†]Molecular Nanophotonics Group, Department and Earth Science, Universität Leipzig, 04103 Leipzig, Germany

[‡]BioNanotechnology and Structure Formation Group, Department of Chemistry and Food Chemistry, Chair of Physical Chemistry, Measurement and Sensor Technology, Technische Universität Dresden, 01062 Dresden, Germany

[§]Kurt-Schwabe-Institut für Mess- und Sensortechnik e.V. Meinsberg, 04736 Waldheim, Germany

Supporting Information

ABSTRACT: We demonstrate a single molecule trapping concept that modulates the actual driving force of Brownian motion—the temperature. By spatially and temporally varying the temperature at a plasmonic nanostructure, thermodiffusive drifts are induced that are used to trap single nano-objects. A feedback controlled switching of local temperature fields allows us to confine the motion of a single DNA molecule for minutes and tailoring complex effective trapping potentials. This new type of thermophoretic microbeaker even provides control over a well-defined number of single molecules and is scalable to large arrays of trapping structures.

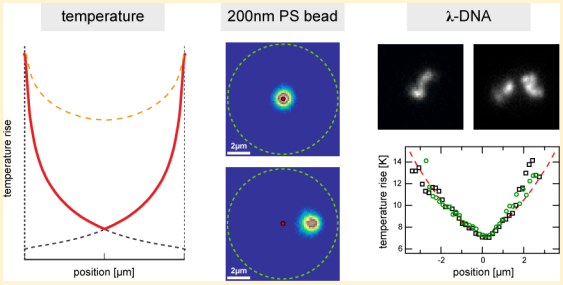

KEYWORDS: *Plasmonics, thermophoresis, Brownian motion, trapping, feedback, nanofluidics*

Since the advent of optical tweezers,[1] the confinement of Brownian motion in fluids has become a powerful tool to investigate processes in soft condensed, biological matter and in fundamental science.[2−4] Scaling this concept of trapping down to hold even single molecules in solution has brought up various tools such as plasmonic tweezers,[5] dielectrophoretic traps,[6] or electrokinetic traps.[7−9] The common concept for trapping of micro- and nano-objects in solution is based on the application of a force which counteracts the thermally driven fluctuations of the object in solution. This force is in general coming from electric fields or field gradients which are set up by focused light,[10] plasmonic near fields,[5] geometry related electrostatic energy landscapes[11] or by applying dynamic electric fields by means of electrode structures as in Paul traps[9] or in the Anti-Brownian Elektrokinetic (ABEL) trap, which combines a feedback mechanism with an actuation by means of electric fields.[7,8]

What has so far not been evaluated for single molecule trapping is the possibility to manipulate the Brownian motion itself using temperature. While an increase of temperature seems at first glance counterintuitive for beating the thermally driven Brownian motion,[12] the related physical effects which are summarized under the term thermophoresis provide a powerful way to control single molecule motion even without making use of convective flows.[13] We show that this scheme even provides routes to confine a well-defined number of single molecules in small regions, paving the way for completely new types of biomolecular interaction dynamics studies on single molecules without surface attachment, which could be advantageously used for example in the field of protein aggregation or enzymatic reactions.

A variation of the local temperature in a material modulates the local thermal equilibrium as thermal energy and the interaction energies compete. This sets up thermally induced currents as observed in many fields of physics as for example the charge current densities in the case of the Seebeck effect or spin current densities in the case of its spin related counterpart.[14] In a solution the current densities correspond to a mass transport of molecules, particles or ions in an inhomogeneous temperature field. This thermodiffusive drift is proportional to the temperature gradient and the thermodiffusion coefficient D_T,[15,16] which is often expressed in terms of the Soret coefficient $S_T = D_T/D$, comparing the strength of thermodiffusion to diffusion. Thermophoresis has been recently applied in various forms for protein binding assays[17] or in combination with convective effects for local molecular concentration enhancement.[18] Recent studies revealed that the microscopic details behind the thermodiffusion are often quite complex and a combination of different contributions.[19,20] For charged species, such as colloids or DNA, electrostatic interactions play a dominant role and temperature gradients result in local electric fields which drive molecular or colloidal motion.[16,19,21] Considering a constant D_T, the Soret coefficient S_T decreases directly proportional with the particles radius, which makes thermophoresis more favorable for trapping small objects than e.g. optical forces relying on polarizability, which

Received: May 21, 2015
Revised: June 29, 2015
Published: July 6, 2015

DOI: 10.1021/acs.nanolett.5b01999
Nano Lett. 2015, 15, 5499−5505

decreases with the particles volume. A similar argument holds for electrokinetic forces used in the ABEL trap.[22]

Independent from the microscopic details that are hidden in the Soret coefficient, the balance of the thermodiffusive and diffusive current densities $-D\vec{\nabla}p - D_T p\vec{\nabla}T = 0$ yields the steady state probability density distribution $p(\vec{r})$ for finding an object at a certain position of the temperature field $T(\vec{r}) = T_0 + \Delta T(\vec{r})$. This probability density is given by the local temperature increment $\Delta T(\vec{r})$ and the Soret coefficient, which is assumed to be temperature-independent.[16,23]

$$p(\vec{r}) = p_0 \exp(-S_T \Delta T(\vec{r})) \quad (1)$$

It follows from eq 1 that an arbitrary temperature profile $\Delta T(\vec{r})$ shall be able to decrease the concentration of the suspended species in regions of high temperature as compared to ambient temperature T_0 as long as S_T is positive. For negative Soret coefficients, hot regions attract the suspended objects. The resulting probability density distribution $p(\vec{r})$ may be represented by an effective potential energy $U_{eff}(\vec{r})$ given by

$$U_{eff}(\vec{r}) = k_B T_0 S_T \Delta T(\vec{r}) \quad (2)$$

This effective potential is different from a "real" potential as in the case of gradient forces in optical or plasmonic tweezers or other trapping systems.[11] Phoretic drifts appear in systems which are force-free and not due to body forces.[24] The here proposed thermophoretic trapping is, therefore, fundamentally different from common trapping schemes. In contrast to many other trapping techniques, the effective potential is also purely repulsive for the most common case of positive Soret coefficients S_T.

According to eq 2, the shape of the temperature profile determines the shape of the effective potential. These temperature profiles may be generated in different ways, e.g., using direct absorption of infrared laser light in water[13,18] or by Joule heating. Here, we rely on simple plasmonic structures prepared by colloidal sphere lithography.[23] The excitation of plasmons on the metal structure allows for an efficient conversion of optical energy into heat. This heat is also present in the case of plasmonic tweezer; however, its effect is typically neglected. As demonstrated below, the effect of the created temperature profile could be very strong. The small spatial extent of the heat source and the large heat bath of the surrounding sample permits to generate high temperature gradients in the order of 10^8 K·m^{-1}, with only a few 10 K of temperature rise at the metal structures. The resulting phoretic drifts have been demonstrated to allow for the trapping of single colloids in stationary temperature fields.[23]

Going beyond this stationary approach and including optical feedback[7] now further increases the temperature gradients while decreasing the temperature increment ΔT at the trapped object. The feedback is thereby realized analyzing the position of the object in the CCD image and steering the heating laser beam at the edge of the plasmonic structure with the help of an acousto-optical deflector (AOD). Since heat diffusion (D_{heat}^{water} = 0.143× 10^6 μm^2/s) is much faster than particle diffusion ($D_{particle}^{water}$ = 2.2 μm^2/s for a ø = 200 nm colloid) temperature fields may be switched very quickly (within microseconds), while the position of the trapped object has effectively not changed.

The advantage of the feedback controlled thermophoretic trapping mechanism is revealed when comparing the static and a feedback controlled temperature field as calculated from finite element simulations (see SI). The shape of the static temperature profile is depicted in Figure 1C as the red dashed line. A relative temperature contrast of about 30% of the maximum temperature rise at the gold structure is found in the static case for a trap diameter of 10 μm. The temperature rise in the center is about 70% of the maximum temperature, which is for most applications unwanted. As compared to this, the temperature profile generated by a single diffraction limited laser spot at the rim of the gold structure is much steeper. This temperature profile is now switched on only at one spot during the exposure to push the trapped object back to the center of the trap in the feedback mode. The spot is selected in a way that the thermophoretic drift is pointing toward the trap center or a target position. The temperature field is thus revolving around the trap center with the tangential diffusion of the object around the center and a feedback time corresponding to the exposure time (τ_{exp} = 10 ms). The effective temperature profile has the shape depicted in Figure 1C as the solid red line. The relative temperature contrast is increased to 86% of the maximum temperature rise and the central temperature at the target position decreases to 14%. This increased temperature contrast yields an improved confinement as readily revealed in the experiment.

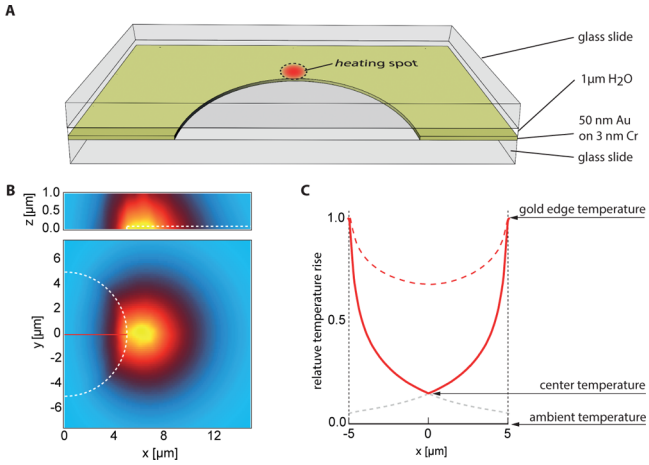

Figure 1. Thermophoretic trap. (A) Scheme of the thermophoretic trap structure consisting of two glass cover slides confining a thin water film of about 1 μm thickness. The lower glass slide carries a thin chromium adhesion layer (3 nm) and a gold layer of 50 nm thickness with a hole of 10−15 μm diameter as prepared by colloidal sphere lithography.[23] A laser beam is illuminating different positions at the rim of the gold structure to generate an inhomogeneous temperature profile. (B) Map of the relative temperature rise generated by a focused laser beam at the rim of the gold structure with 10 μm diameter (dashed) in the plane of the gold film as calculated from finite element simulations. The top image shows the temperature rise across the liquid film. (C) Calculated relative temperature rise profile in the thermophoretic trap. The temperature rise is scaled to the maximum temperature rise at the gold structure. The red dashed line corresponds to the steady state temperature profile if the whole gold structure is heated. The solid line depicts the effective temperature profile, which is established when the feedback mode with trapping target at x = 0 μm is used. The gray dashed line extends the red solid line in the case the gold film is heated at just one spot without position feedback.

The experimental setup comprises a conventional inverted microscope with an acousto-optical deflector as a beam steering unit for the heating laser (see Figure 1A and Methods section

DOI: 10.1021/acs.nanolett.5b01999
Nano Lett. 2015, 15, 5499−5505

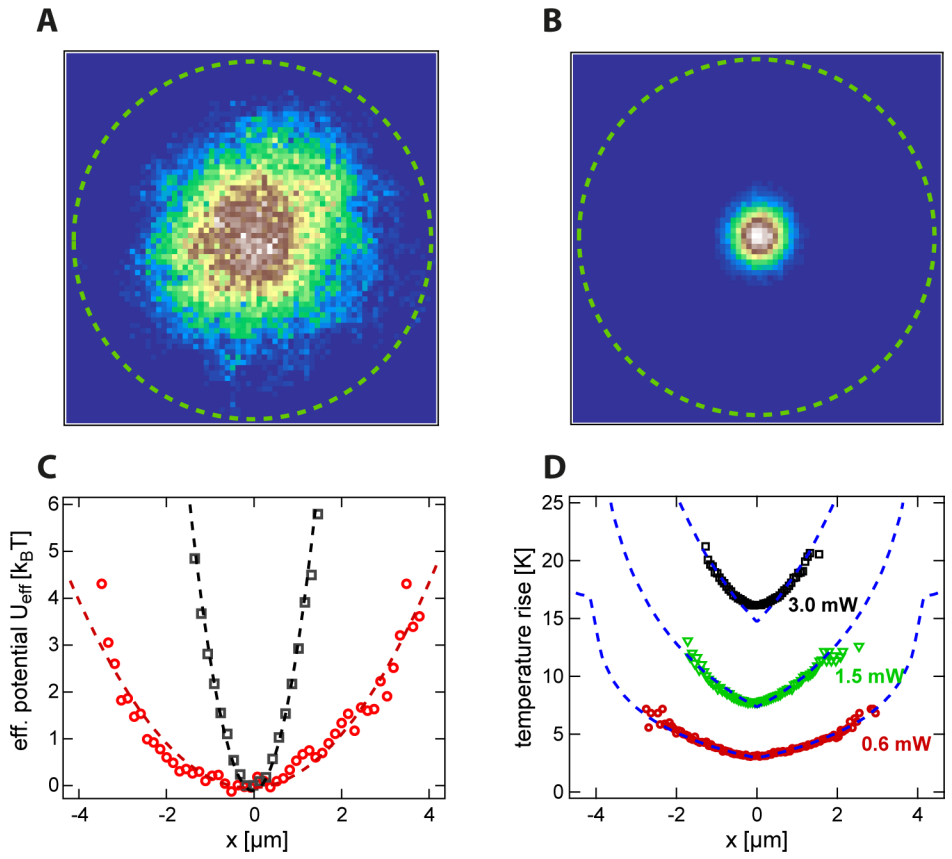

Figure 2. Comparison of steady state and feedback trapping. (A) Probability density of finding a ø = 200 nm polystyrene colloid inside the trapping region for a steady state temperature profile and (B) for feedback controlled trapping for an incident heating power of 3.0 mW focused to a diffraction limited spot at the gold film. Trap diameter d_{trap} = 10 μm with the dashed lines indicating the trap edge. (C) Comparison of the effective potentials generated as calculated from $U_{eff} = -k_B T_0 \ln(p(x))$. The red dots correspond to the experimental data obtained for the steady state temperature field with a parabolic fit (red line). The black symbols correspond to the feedback trapping results. (D) Temperature profiles reconstructed from the position distribution $p(x)$ and the diffusion coefficient of the ø = 200 nm colloid measured at different heating power for the feedback mode. The dashed lines correspond to the relative temperature increments of Figure 1C scaled by the temperature rise at the heated spot on the gold film. (Trap diameter d_{trap} = 8.3 μm.)

for details). The sample consists of two glass cover slides where the lower one carries the gold structure and the liquid film between the slides, which is of about 1 μm thickness. The quasi-static temperature field is generated by a laser focus quickly rotating around the trapping gold structure (at about 100 Hz). This gives rise to an effective temperature field, which corresponds to the static temperature profile in Figure 1B,C.[25]

Figures 2A and B display the obtained probability density distributions for finding a single colloid of 200 nm diameter in the trap (d_{trap} = 10 μm, dashed line in top images) for the same heating laser intensity (3.0 mW focused to a diffraction limited spot of ø = 1 μm) for quasi-static and feedback controlled heating. The distribution is in both cases well represented by a Gaussian. The width of the Gaussian in the feedback mode has decreased by a factor of 3.5 as compared to the quasi-static heating, which corresponds to an increase by a factor of 12 in terms of trapping stiffness (κ_{FB} = 22 fN·μm^{-1} vs κ_{QS} = 1.9 fN·μm^{-1}). In all of the presented studies, the stiffness of the trap as defined by the curvature of the potential is low as compared to optical tweezers. Trapping stiffness, however, becomes relevant when measuring forces with the help of the trap. As the main objective of our trap is the confinement of objects for extended time periods, the stiffness is less important.

Due to the higher temperature gradients generated in the feedback mode, the particle can effectively be trapped at lower temperature. The temperature profile can be reconstructed using the temperature dependence of the diffusion coefficient and the positional distribution (see SI). As the probability for finding the particle is highest in the center of the structure, its average temperature is well-approximated by the temperature in the trap center.[23] Measuring the increase of the average diffusion coefficient as a function of the heating power reveals a temperature increase per incident heating power of 5.4 K/mW in the center (trap diameter d_{trap} = 8.3 μm) and 29 K/mW at the gold structure. The calculated relative temperature profiles can thus be scaled to the gold structure temperature value and compared to the logarithm of the probability density distribution of the particle in the trap as shown in Figure 2D. Both calculated and measured temperature profiles agree well and yield a Soret coefficient of S_T = 1.5 K^{-1} at all studied heating powers. This Soret coefficient compares well to literature values.[15] Note that the average temperature rise in the center decreases with increasing trap diameter (see SI). The average temperature increase in Figure 1A and B was about 13 K. By using less heating laser power and the feedback scheme, the same confinement as in Figure 1A may be achieved with only an average temperature rise of about 1 K.

While the 200 nm colloid can be virtually trapped forever, the limits of the trapping scheme are given by the Soret coefficient and the shape of the temperature field. If the width

DOI: 10.1021/acs.nanolett.5b01999
Nano Lett. 2015, 15, 5499−5505

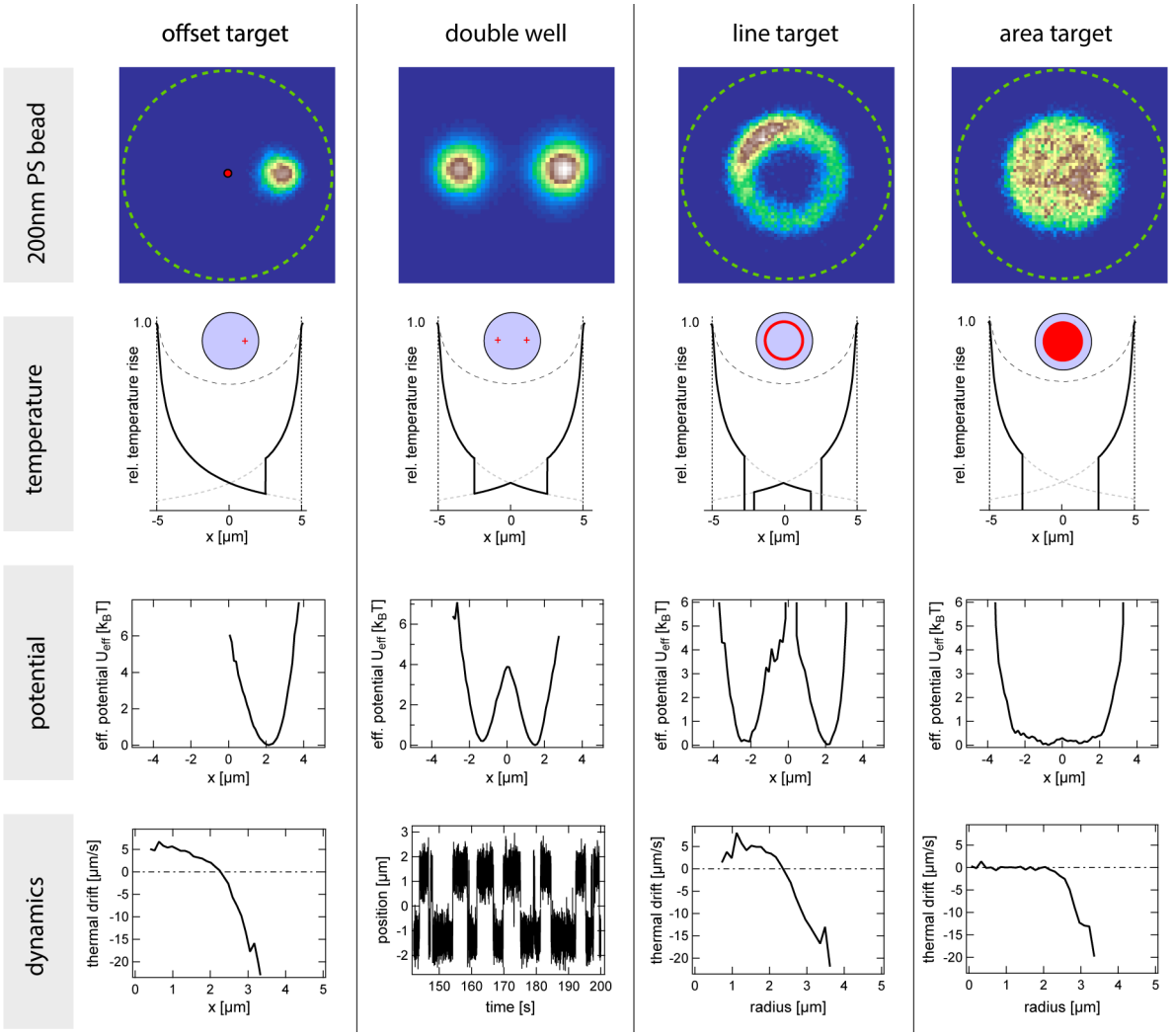

Figure 3. Shaping effective trapping potentials. Examples of different effective trapping potential landscapes generated by different feedback rules for a single ø = 200 nm colloid in a d_{trap} = 10 μm trap at 3.0 mW heating laser power. The individual rows display the probability density distribution of the particle in the trap, the calculated relative temperature rise along the horizontal cross section in comparison with the steady state temperature profile, the effective potential profile along the horizontal cross section as calculated from the probability distribution in the top row, and the drift speed as determined along the horizontal cross section calculated from the single particle trajectories. For the double well potential the hopping of the colloid between the different potential minima is depicted.

of the distribution given by eq 1 exceeds the radius of the trapping structure, objects cannot be stably trapped. In all other cases, the average trapping time τ may be accessed by adopting Kramers theory as described in the Supporting Information. This calculation yields

$$\tau = \frac{2\pi}{D_T} \frac{1}{\Delta T_{max}\sqrt{\alpha'(a)|\alpha'(b)|}} e^{S_T \Delta T_{max}} \quad (3)$$

where $\alpha' = \alpha/\Delta T_{Au}$ is the curvature of the temperature field at the potential minimum position a and the potential maximum position b normalized to the temperature at the heated spot ΔT_{Au}. The main contribution in eq 3 comes from the last term, which increases the trapping duration exponentially with S_T and the temperature contrast ΔT_{max} between the center and the edge of the trap structure. Using the current setup, we were able to trap colloids as small as ø = 28 nm for several tens of seconds in water (see SI). The Soret coefficient of these colloids was about $S_T \approx 0.13$ K^{-1}, which is comparable to double-stranded DNA of a few 100 base pairs in length.[26,27]

The experimental scheme so far has employed only a single point target located at the center of the trap. In general, the feedback rule used for the trapping can be designed in an almost arbitrary way. Similar as for the ABEL trap,[28,29] the target position neither has to be in the center of the trap nor it has to be a single point target. To demonstrate the versatility of the trapping scheme, we have realized several other trapping targets. A few examples are depicted in Figure 3. The figure displays the density distributions $p(\vec{r})$, the corresponding calculated temperature along the horizontal axis, the extracted effective potentials U_{eff}, and the dynamics of the colloid in the trap in the different rows. The first column exhibits the results for a point-like target offset from the center of the trapping region. Note that the temperature profile now shows a jump at the target position, which has no consequence on the trapping potential as the particle motion is governed by either the temperature gradient left or right of the target position, which shows a jump at off-center target that is blurred by Brownian motion. Also, multiple point-like targets may be defined, which resemble an effective double well potential as displayed in the

DOI: 10.1021/acs.nanolett.5b01999
Nano Lett. 2015, 15, 5499−5505

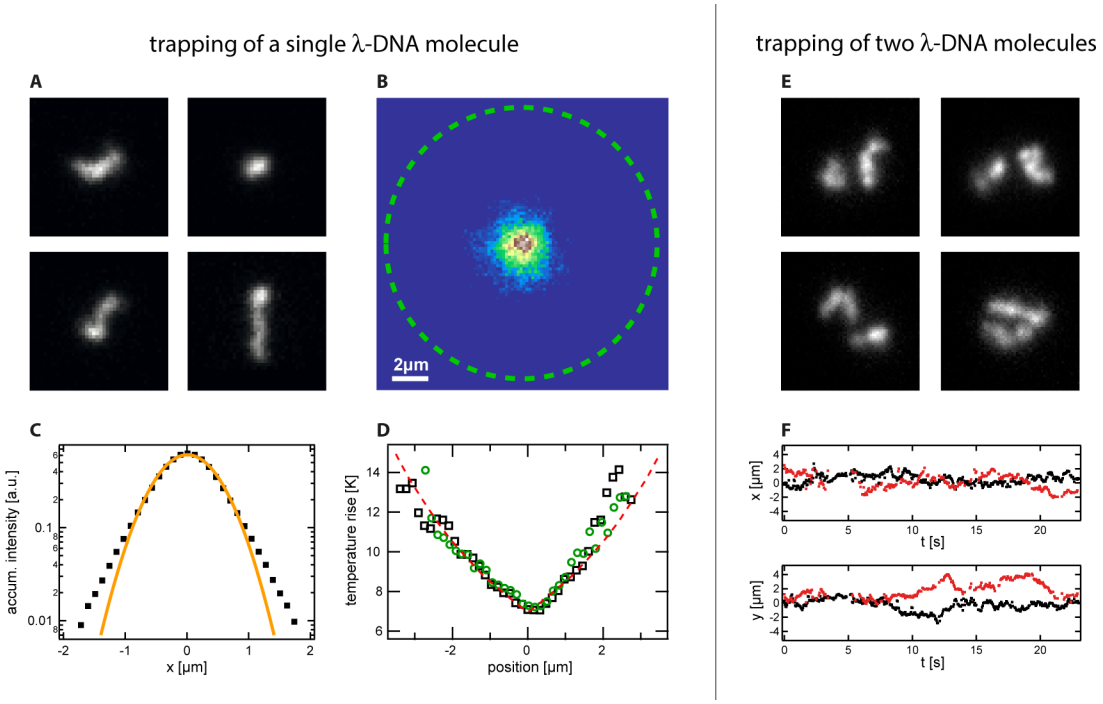

Figure 4. Thermophoretic trapping of λ-DNA molecules. (A) Four snapshots ($4.6 \times 4.6\ \mu m^2$) of a trapped single λ-DNA molecule. (B) Probability density of the trapped molecule with a width $\sigma = 0.75\ \mu m$ at 3.0 mW heating laser power. (C) Accumulated fluorescence intensity after shifting each frame by the molecules center of mass and normalization, showing a nongaussian mass distribution about the center of mass. Gaussian fit in orange ($R_G = (0.66 \pm 0.02)\ \mu m$). (D) Temperature field in the trap reconstructed from the probability density of the molecule in x (black) and y (green) direction for a measured Soret coefficient of $S_T = 0.8\ K^{-1}$ and theoretical temperature field (red dashed curve). (E) Four snapshots ($6.9 \times 6.9\ \mu m^2$) of the trapping of two single λ-DNA molecules. (F) x and y components of the trajectories of the two DNA molecules trapped in a $d_{trap} = 15\ \mu m$ trap.

second column. The distance of the particle from the individual trapping sites then decides to which target the particle is pushed. The corresponding hopping dynamics is revealed in Figure 3, and its statistics follow Kramers theory as expected for a real potential energy landscape even though there is no potential present in our case. The trapping potential may also be shaped as a quasi 1-dimensional potential ring allowing for a circular diffusion, which provides the perspective to study complex ratchet like transport behavior under additional external modulation. Finally, also an area target may be defined, where the object is freely diffusing without any temperature increase as long as it is within a certain distance from the trap center. This box-like potential generates the smallest possible temperature perturbation to the trapped object and allows studies at ambient temperature.

The performance of the thermophoretic feedback trap allows us to confine single macromolecules using the processes induced by the inhomogeneous temperature field. Figure 4A shows example images from a 500 s long timetrace of a λ-DNA molecule recorded at an inverse framerate of 50 ms (see SI for movie) and a heating power of 3.0 mW. The trapping duration is limited by the bleaching of the dye molecules in this experiment. The position distribution in Figure 4B reveals a confinement of the molecule to a spatial dimension of $\sigma = 0.75$ μm as determined from the fluctuations of the center of intensity of the molecule in the trap. Overall more than 10 different DNA molecules have been studied for shorter periods at a higher time resolution of 10 ms per frame. The single molecule images allow for an analysis of conformational fluctuations. As described previously for λ-DNA in the ABEL trap,[30] the conformation deviates from a Gaussian chain as indicated by the average intensity image of the molecule with respect to its center of intensity (Figure 4C). Figure 4D shows the corresponding temperature distribution in the trap reconstructed from the position distribution of the molecule with a measured Soret coefficient of $S_T = 0.8\ K^{-1}$, which compares well to experiments by Duhr and Braun.[27] A more detailed analysis of the DNA conformation in the trap shows that there is no detectable perturbation of the molecular conformation in the trap at the heating powers used in the experiment (see SI). According to the temperature profiles expected, the temperature difference over the radius of gyration of the molecule ($R_G = 0.66\ \mu m$) is below 0.1 K. The molecule thus essentially feels an isothermal environment. As the temperature field in the trap is inhomogeneous, however, it is expected that smaller trap structures cause stronger temperature differences over the extent of the DNA, and thus, may compress the conformation. As a recent report has demonstrated that the DNA thermophoresis at low ionic strength is largely governed by local electric fields generated by the temperature gradients,[19] a more detailed analysis of the conformation dynamics or even the thermophoretic drift of different molecular sites may give new information on the fundamental physics of thermophoresis.[31]

While the experiments described above have demonstrated the versatility of the feedback mode to design different trapping potentials for single nano-objects including single molecules, our thermophoretic trap is capable of confining a controlled number of objects. Thus, molecular interactions can be studied at low enough concentration to be able to discern single molecules, but still with a large probability of molecular encounters which would typically only be possible at very high

DOI: 10.1021/acs.nanolett.5b01999
Nano Lett. 2015, 15, 5499−5505

concentrations. This strategy may therefore simulate physiological concentrations, i.e., in protein aggregation assays without actually heaving them.

A controlled trapping of multiple objects is not possible in trapping schemes using homogeneous fields.[7] Trapping of multiple objects of micrometer size in larger traps has been demonstrated by dedicated multimodal electroosmotic flow fields produced by a many electrode system[32,33] and an advanced feedback algorithm.[34] The ability to study a controlled number of nano-objects in the thermophoretic trap comes due to the fact that the generated phoretic drift is inhomogeneous within the trap and objects close to the heated spot experience a larger displacement than objects farther away. Objects are therefore pushed toward each other if the feedback is set to respond to a well-defined number of objects (see SI). Further, the effective trapping potentials are repulsive for a positive Soret coefficient. Thus, if the trapping of two or more objects or molecules is achieved, no other molecules would enter the trap as they are repelled from the trap structure as well.

These advantages are demonstrated by trapping two DNA molecules with a single target in the center of the trap. Figure 4E shows four snapshots of a 30 s long trajectory of two DNA molecules in a d_{trap} = 15 μm trap. The corresponding traces of the x and y position in the sample plane are given in Figure 4F. The confinement if two DNA molecules are trapped is slightly weaker than for a single DNA. This is due to the fact that the heating spot is positioned in a way that one molecule is radially pushed toward the target, while the thermophoretic drift for the other molecule is not pointing toward it. This effect can be minimized by optimizing the heating positions to avoid this cross-talk. Further, multicolor experiments may be carried out to image different species at different colors to resolve even very close encounters. For all of these trapped species, one would then be able to analyze the diffusive and thermodiffusive mobilities, which allows getting insight into binding or aggregation dynamics where commonly only kinetics can be accessed.[8] In case of molecular species with different Soret coefficient, the heating power can be modified when actuating the individual molecules to correct for the differences in the phoretic mobility. Combined with the shaping of the effective potential as described above, the thermophoretic trap as presented here may store and manipulate molecules in a small trapping region to allow for completely new experiments, which could for example shed new light on the dynamics of protein aggregation in amyloid formation.[35]

The possibility of trapping single molecules just by the action of dynamic temperature fields in solution presents a new way of manipulating molecules not by external body forces, but with the help of the fuel that drives its fluctuations. This type of trapping, which is fundamentally different from the commonly used trapping, presents a variety of perspectives of handling single and even multiple macromolecules in a very simple way. As colloidal sphere lithography easily delivers large arrays of plasmonic trapping structures, the technique is easily scalable to many trapping structures where transport between individual traps may be realized. In this way, thermophoretic single molecule trapping can readily find applications in the field of enzymatic reactions,[36] protein binding,[17] or protein aggregation.[35] The ability to trap single macromolecules such as DNA with well-defined temperature gradients on the other side also allows to tackle new fundamental problems of nonequilibrium physics.[31,37] We therefore expect this tool to find broad applications in soft condensed matter, biophysics, and pharmaceutical research.

Methods. The experimental setup is build around an inverted widefield fluorescence microscope (Olympus lens 100/NA1.3, Andor Ixon EMCCD camera, typically used at a framerate of 100 Hz and 2 × 2 pixel binning). Brightfield illumination is used to adjust the gold structure in the field of view. An expanded 532 nm-wavelength laser beam ($\omega_{0,w} \approx 20$ μm) is used to excite fluorescence. An additional focused 532 nm laser beam ($\omega_{0,h} \approx 1$ μm) can be steered within the sample plane by means of an 2D-acousto-optic deflector (Brimrose) to heat the gold structure locally. Particle or molecule positions are tracked in real-time by a LabView program and are used by an AD/DA converter (ADwin-Gold II, Jäger Messtechnik GmbH) to control the acousto-optic deflector (AOD, Brimrose) by applying according feedback rules to heat a particular position on the gold structure.

Materials. Clean glass cover slides are coated with a 3 nm chromium adhesion layer. Isolated PS microparticles (8−15 μm, Microparticles GmbH) are spin-coated onto the chromium layer. A 50 nm gold film is evaporated on top followed by a removal of the PS particles by ultrasonic treatment. The uncovered chromium film is removed by etching. In the experiments, a second glass slide confines a water film of about 700 nm to 1 μm in height. The water film contains either fluorescent colloidal particles (200 nm, Invitrogen FluoSpheres, stock solution diluted with deionized water) or POPO3-labeled λ-DNA (in 3 mM phosphate buffer). The glass and gold surfaces are passivated by Pluronic F-127 (Sigma-Aldrich) to avoid sticking of the colloids or DNA.

λ-DNA (NEB, N3011) with a contour length of 16.3 μm was stained with the bisintercalating fluorescence dye POPO-3 (life technologies, P3584) at a ratio 1 dye/8 base pairs in 100 mM phosphate buffer (sodium phosphate buffer: 18.8 mM $NaH_2PO_4 \cdot H_2O$, 81.3 mM $Na_2HPO_4 \cdot 2H_2O$, resulting in a pH of 7.5) at a final DNA concentration of 1.28 nM. The mixture was incubated for at least 1 h at 50 °C in order to ensure homogeneous staining. The contour length of the DNA is expected to increase to approximately 19 μm due to intercalation of POPO-3. For the trapping experiments the DNA was further 30-fold diluted with H_2O.

■ ASSOCIATED CONTENT

Supporting Information

A detailed description of the feedback control, the simulation of the temperature fields, a calculation of the temperature dependent diffusion coefficient, the mean squared displacement of a trapped particle and the experimental setup. Several movies visualizing the different trapping modes. The Supporting Information is available free of charge on the ACS Publications website at DOI: 10.1021/acs.nanolett.5b01999.

■ AUTHOR INFORMATION

Corresponding Author

*E-mail: cichos@physik.uni-leipzig.de.

Notes

The authors declare no competing financial interest.

■ ACKNOWLEDGMENTS

We acknowledge the support of the Collaborative Research Project TRR 102 “Polymers under Multiple Constraints”, the DFG Research Unit 877 “From Local Constraints to

DOI: 10.1021/acs.nanolett.5b01999
Nano Lett. 2015, 15, 5499−5505

Macroscopic Transport", the DFG priority program 1726 "Microswimmers" as well as funding by the European Union and the Free State of Saxony. Also, financial support by the graduate school BuildMoNa, by the Cluster of Excellence "cfaed" (EXC1056/1) and the ESF project MindNano (100111059) are acknowledged.

REFERENCES

(1) Ashkin, A.; Dziedzic, J. M.; Bjorkholm, J. E.; Chu, S. *Opt. Lett.* **1986**, *11*, 288−290.
(2) Grier, D. G. *Nature* **2003**, *424*, 810−816.
(3) Bohlein, T.; Mikhael, J.; Bechinger, C. *Nat. Mater.* **2011**, *11*, 126−130.
(4) Kheifets, S.; Simha, A.; Melin, K.; Li, T.; Raizen, M. G. *Science* **2014**, *343*, 1493−1496.
(5) Juan, M. L.; Righini, M.; Quidant, R. *Nat. Photonics* **2011**, *5*, 349−356.
(6) Hölzel, R.; Calander, N.; Chiragwandi, Z.; Willander, M.; Bier, F. *Phys. Rev. Lett.* **2005**, *95*, 128102.
(7) Cohen, A. E.; Moerner, W. E. *Proc. Natl. Acad. Sci. U. S. A.* **2006**, *103*, 4362−4365.
(8) Wang, Q.; Moerner, W. E. E. *Nat. Methods* **2014**, *11*, 555−558.
(9) Guan, W.; Joseph, S.; Park, J. H.; Krstić, P. S.; Reed, M. A. *Proc. Natl. Acad. Sci. U. S. A.* **2011**, *108*, 9326−9330.
(10) Hansen, P. M.; Bhatia, V. K.; Harrit, N.; Oddershede, L. *Nano Lett.* **2005**, *5*, 1937−1942.
(11) Krishnan, M.; Mojarad, N.; Kukura, P.; Sandoghdar, V. *Nature* **2010**, *467*, 692−695.
(12) Rings, D.; Schachoff, R.; Selmke, M.; Cichos, F.; Kroy, K. *Phys. Rev. Lett.* **2010**, *105*, 090604.
(13) Weinert, F. M.; Braun, D. *Nano Lett.* **2009**, *9*, 4264−4267.
(14) Uchida, K.; Takahashi, S.; Harii, K.; Ieda, J.; Koshibae, W.; Ando, K.; Maekawa, S.; Saitoh, E. *Nature* **2008**, *455*, 778.
(15) Duhr, S.; Braun, D. *Phys. Rev. Lett.* **2006**, *97*, 038103.
(16) Würger, A. *Rep. Prog. Phys.* **2010**, *73*, 126601.
(17) Wienken, C. J.; Baaske, P.; Rothbauer, U.; Braun, D.; Duhr, S. *Nat. Commun.* **2010**, *1*, 100.
(18) Mast, C. B.; Braun, D. *Phys. Rev. Lett.* **2010**, *104*, 188102.
(19) Reichl, M.; Herzog, M.; Götz, A.; Braun, D. *Phys. Rev. Lett.* **2014**, *112*, 198101.
(20) Fayolle, S.; Bickel, T.; Wurger, A. *Phys. Rev. E* **2008**, *77*, 041404.
(21) Piazza, R.; Parola, A. J. *J. Phys.: Condens. Matter* **2008**, *20*, 153102.
(22) Cohen, A. E.; Moerner, W. E. *Appl. Phys. Lett.* **2005**, *86*, 093109.
(23) Braun, M.; Cichos, F. *ACS Nano* **2013**, *7*, 11200.
(24) Jülicher, F.; Prost, J. *Eur. Phys. J. E: Soft Matter Biol. Phys.* **2009**, *29*, 27−36.
(25) Braun, M.; Würger, A.; Cichos, F. *Phys. Chem. Chem. Phys.* **2014**, *16*, 15207.
(26) Duhr, S.; Arduini, S.; Braun, D. *Eur. Phys. J. E: Soft Matter Biol. Phys.* **2004**, *15*, 277−86.
(27) Duhr, S.; Braun, D. *Proc. Natl. Acad. Sci. U. S. A.* **2006**, *103*, 19678−19682.
(28) Cohen, A. E. *Phys. Rev. Lett.* **2005**, *94*, 118102.
(29) Gavrilov, M.; Jun, Y.; Bechhoefer, J. *Rev. Sci. Instrum.* **2014**, *85*, 095102.
(30) Cohen, A. E.; Moerner, W. E. *Phys. Rev. Lett.* **2007**, *98*, 116001.
(31) Pedersen, J. N.; Lüscher, C. J.; Marie, R.; Thamdrup, L. H.; Kristensen, A.; Flyvbjerg, H. *Phys. Rev. Lett.* **2014**, *113*, 268301.
(32) Armani, M. D.; Chaudhary, S. V.; Probst, R.; Shapiro, B. *J. Microelectromech. Syst.* **2006**, *15*, 945−956.
(33) Probst, R.; Cummins, Z.; Ropp, C.; Waks, E.; Shapiro, B. *IEEE Control Syst.* **2012**, *32*, 26−53.
(34) Chaudhary, S.; Shapiro, B. *IEEE Trans. Control Syst. Technol.* **2006**, *14*, 669−680.
(35) Dobson, C. M. *Nature* **2003**, *426*, 884−890.
(36) Arenkov, P.; Kukhtin, A.; Gemmell, A.; Voloshchuk, S.; Chupeeva, V.; Mirzabekov, A. *Anal. Biochem.* **2000**, *278*, 123−31.
(37) Otto, O.; Sturm, S.; Laohakunakorn, N.; Keyser, U. F.; Kroy, K. *Nat. Commun.* **2013**, *4*, 1780.

DOI: 10.1021/acs.nanolett.5b01999
Nano Lett. 2015, 15, 5499−5505